

## Probing the Hofstadter butterfly with the quantum oscillation of magnetization

W. H. Xu,<sup>1</sup> L. P. Yang,<sup>1,\*</sup> M. P. Qin,<sup>2</sup> and T. Xiang<sup>1,2</sup>

<sup>1</sup>*Institute of Theoretical Physics, Chinese Academy of Sciences, P.O. Box 2735, Beijing 100190, China*

<sup>2</sup>*Institute of Physics, Chinese Academy of Sciences, P.O. Box 603, Beijing 100190, China*

(Received 16 November 2008; published 18 December 2008)

We have developed a different quantum transfer-matrix method to accurately determine thermodynamic properties of the Hofstadter model. This method resolves a technical problem which is intractable by other methods and makes the calculation of physical quantities of the Hofstadter model in the thermodynamic limit at finite temperatures feasible. It is shown that the quantum correction to the de Haas–van Alphen oscillation of magnetization bears the energy structure of the Hofstadter butterfly. The measurement of this quantum correction, which can be materialized on the superlattice or cold atom systems, can reveal unambiguously the Hofstadter fractal energy spectrum.

DOI: 10.1103/PhysRevB.78.241102

PACS number(s): 71.10.Fd, 05.30.Fk, 75.20.-g

The Hofstadter butterfly is the fractal phase diagram of crystalline electrons in a magnetic field.<sup>1,2</sup> This problem is of particular interest because it is one of the few examples in physics where the difference between rational and irrational numbers can be tested by experimental measurements.<sup>3–5</sup> However, probing the Hofstadter butterfly is a challenging problem because a tiny change in the external magnetic field may give rise to radical reconstructions of the ground state. Some hints of the Hofstadter butterfly were reported in quantum hall conductivity,<sup>5</sup> magnetic transport,<sup>6</sup> and microwave<sup>7</sup> measurements.

The Hofstadter butterfly results from the interplay between a uniform magnetic field and a periodic crystal potential of two-dimensional electron gas. Thirty years ago, Hofstadter<sup>2</sup> computed the energy spectrum of the Harper equation<sup>8</sup> and discovered this fractal butterfly structure as a function of the magnetic flux per lattice cell  $\phi$ . The Hofstadter model has become a paradigm for quantum systems with singular continuous spectra and nontrivial topological numbers. This model has been solved by the Bethe ansatz<sup>9,10</sup> and exact diagonalization<sup>11</sup> methods when  $\phi$  is rational  $\phi = p/q$  ( $p$  and  $q$  are mutually prime integers) with relatively small  $q$ .

Previous studies of the Hofstadter model have focused on the ground state. There was also a discussion on the magnetization oscillation with the chemical potential at zero temperature.<sup>12</sup> As the ground-state energy is not an analytic function of applied magnetic field due to the fractal feature of spectra, the magnetic susceptibility is not a well-defined quantity at zero temperature. Thermal fluctuation can smear the singularity and remove this nonanalytical feature. However, to study thermodynamic properties at finite temperatures, especially the lattice correction to the quantum oscillation of magnetization as a function of magnetic field, one has to solve this model for arbitrary  $\phi$ . This is a very challenging problem since the largest  $q$  that can be handled by the Bethe ansatz or exact diagonalization is generally less than 1000.

In this Rapid Communication, we propose a different quantum transfer-matrix method to study thermodynamic properties of the Hofstadter model on square lattices. This method avoids direct diagonalization of the Hamiltonian and allows the thermodynamic limit to be explored directly and

accurately. In Ref. 13, magnetic quantum oscillations were obtained. We will show that the quantum oscillation of magnetization is a susceptible physical quantity to probe the hierarchical structure of the Hofstadter butterfly. The measurement of the quantum oscillation of magnetization reveals unambiguously the Hofstadter's fractal energy spectrum.

Let us start by taking the Landau gauge in which the vector potential to be zero along the  $x$  axis. By further taking the plane-wave expansion along the  $x$  axis, we then decouple the Hofstadter model  $H$  into a sum of a series of one-dimensional Hamiltonian  $H_k$ ,

$$H = \sum_k H_k, \quad (1)$$

$$H_k = \sum_y [t c_{k,y+1}^\dagger c_{k,y} + t c_{k,y}^\dagger c_{k,y+1} + 2t \cos(2\pi y \phi - k) c_{k,y}^\dagger c_{k,y}], \quad (2)$$

where  $k = 2\pi n/N_x$  ( $n = 0, 1, \dots, N_x - 1$ ) is the momentum of electrons along the  $x$  axis and  $N_x$  is the lattice dimension along that direction.  $y$  is the lattice coordinate of electrons along the  $y$  axis.  $\phi$  is the magnetic flux penetrating each plaquette.

Given  $k$ , the partition function of  $H_k$  is defined by

$$Z_k = \text{Tr} \exp(-\beta H_k), \quad (3)$$

where  $\beta = 1/k_B T$  and  $T$  is temperature. The partition function of the whole system is simply a product of  $Z_k$  for all  $k$ .

To evaluate  $Z_k$ , let us first divide  $H_k$  into two parts,  $H_k = H_{k,\text{even}} + H_{k,\text{odd}}$ , where

$$H_{k,\text{odd}} = \sum_y h_{k,2y-1},$$

$$H_{k,\text{even}} = \sum_y h_{k,2y},$$

and

$$h_{k,y} = t(c_{k,y+1}^\dagger c_{k,y} + \text{H.c.}) + 2t \cos(2\pi y \phi - k) c_{k,y}^\dagger c_{k,y}.$$

The individual terms  $h_{k,y}$  in  $H_{k,\text{even}}$  or  $H_{k,\text{odd}}$  commute with each other. Thus it is relatively simple to evaluate thermody-

dynamic quantities of  $H_{k,\text{even}}$  or  $H_{k,\text{odd}}$ . To utilize this property, let us divide  $\beta$  into  $M$  equivalent parts  $\varepsilon = \beta/M$  and apply the Trotter-Suzuki formula<sup>14,15</sup> to decompose  $Z_k$  as

$$Z_k = \text{Tr}(e^{-\varepsilon H_{k,\text{odd}}} e^{-\varepsilon H_{k,\text{even}}})^M + O(\varepsilon^2). \quad (4)$$

By inserting completeness identities to the above expression, we have

$$Z_k = \lim_{\varepsilon \rightarrow 0} \prod_{l=1}^M \prod_{y=1}^{N_y/2} v_{2y-1,2y}^{2l-1,2l} v_{2y,2y+1}^{2l,2l+1}, \quad (5)$$

where

$$v_{y,y+1}^{l,l+1} = \langle n_y^l n_{y+1}^l | e^{-\varepsilon h_{k,y}} | n_y^{l+1} n_{y+1}^{l+1} \rangle. \quad (6)$$

The subscripts represent the lattice positions and the superscripts represent the coordinates in the inverse temperature or Trotter space.

From Eq. (6), one can define a local transfer operator  $\tau$  whose matrix elements are given by

$$\tau_{y,y+1}^{l,l+1} = \langle n_y^l, 1 - n_y^{l+1} | e^{-\varepsilon h_{k,y}} | 1 - n_{y+1}^l, n_{y+1}^{l+1} \rangle. \quad (7)$$

An important step in the calculation below is to define this local transfer matrix using fermion operators. Through a tedious calculation, we find that this transfer matrix can be expressed as an exponent of a quadratic function of fermion operators,

$$\tau_{y,y+1}^{l,l+1} = u_{k,y} \exp[p_{k,y} d_l^\dagger d_{l+1} + q_{k,y} d_{l+1}^\dagger d_l + r_{k,y} (d_l^\dagger d_l - d_{l+1}^\dagger d_{l+1})], \quad (8)$$

where  $d$ 's are fermion operators defined in the Trotter space and coefficients  $(p_{k,y}, q_{k,y}, r_{k,y})$  are determined by the following equations:

$$\frac{\sinh s_{k,y}}{s_{k,y}} p_{k,y} = -\frac{\gamma_{k,y} \exp(\alpha_{k,y})}{\varepsilon t \sinh \gamma_{k,y}},$$

$$\frac{\sinh s_{k,y}}{s_{k,y}} q_{k,y} = -\frac{\gamma_{k,y} \exp(-\alpha_{k,y})}{\varepsilon t \sinh \gamma_{k,y}},$$

$$\frac{\sinh s_{k,y}}{s_{k,y}} r_{k,y} = -\frac{\alpha_{k,y}}{\varepsilon t},$$

$\alpha_{k,y} = -\varepsilon [t \cos(2\pi y \phi - k) - \mu/2]$ ,  $\gamma_{k,y} = \sqrt{\alpha_{k,y}^2 + \varepsilon^2 t^2}$ ,  $u_{k,y} = -\varepsilon t \sinh \gamma_{k,y} \exp(\alpha_{k,y}) / \gamma_{k,y}$ , and  $s_{k,y} = \sqrt{p_{k,y} q_{k,y} + r_{k,y}^2}$ .  $\mu$  is the chemical potential. In general, for any quadratic Hamiltonian, it can be shown that the corresponding local transfer matrix can be always written as an exponent of a quadratic function of fermion operators.<sup>16</sup>

Reversing the order of  $l$  and  $y$  in Eq. (5), one can then re-express the partition function as a product of transfer matrices,

$$Z_k = \lim_{\varepsilon \rightarrow 0} \text{Tr}(T_{1,2} T_{2,3} \cdots T_{N,1}), \quad (9)$$

where  $T_{y,y+1}$  are transfer operators defined by

$$T_{2y-1,2y} = \prod_l v_{2y-1,2y}^{2l-1,2l},$$

$$T_{2y,2y+1} = \prod_l v_{2y,2y+1}^{2l,2l+1}.$$

Since coefficients  $(p_{k,y}, q_{k,y}, r_{k,y})$  do not depend on  $l$ , the above transfer operators are translationally invariant in every two unit cells along the Trotter direction. Thus we can block diagonalize these transfer matrices by taking the Fourier transformation of fermion operators in the Trotter space. Finally, we find that in the thermodynamic limit  $Z_k$  can be expressed as a product of  $N_y$   $2 \times 2$  matrices given by the following formula:

$$Z_k = \lim_{\varepsilon \rightarrow 0} \text{Tr} \prod_{\omega} \prod_y^{N_y/2} [t_{k,2y-1}^-(\omega) t_{k,2y}^+(\omega)], \quad (10)$$

where  $\omega = (2m+1)\pi/M$  ( $m=1, \dots, M$ ) is the imaginary frequency.  $t_{k,y}^\pm(\omega)$  are  $2 \times 2$  matrices defined by

$$t_{k,y}^\pm(\omega) = u_{k,y} \begin{pmatrix} a_{k,y}^\pm & e^{-i\omega} b_{k,y}^\pm \\ e^{i\omega} b_{k,y}^\mp & a_{k,y}^\mp \end{pmatrix}, \quad (11)$$

where

$$a_{k,y}^\pm = \frac{\gamma_{k,y} \cosh \gamma_{k,y} \pm \alpha_{k,y} \sinh \gamma_{k,y}}{-\varepsilon t \sinh \gamma_{k,y}},$$

$$b_{k,y}^\pm = \frac{\gamma_{k,y} \exp(\pm \alpha_{k,y})}{-\varepsilon t \sinh \gamma_{k,y}}.$$

Thus the partition function can be obtained simply by computing the product of a number of  $2 \times 2$  matrices. This is a great simplification to the problem, since the computer time needed scales just linearly with  $N_y$ . Furthermore, we need not store all these transfer matrices in advance. The computer memory needed in the calculation is very small. Thus a truly big system with  $N_y \sim 10^8$  can be handled without any technical obstacle.

From the partition function, one can readily calculate the free energy of the system  $F = -\frac{1}{\beta} \ln Z$ . The magnetization and magnetic susceptibility can then be determined numerically from the first and second derivatives of the free energy with respect to the applied magnetic field.

In the Landau gauge, the lattice rotational symmetry is broken. The finite-size effect along the  $x$  direction is small. In the temperature range considered, we find that  $N_x = 50$  is large enough. However, along the  $y$  axis, the finite-size effect is strong. By evaluating the magnetization at  $T = 0.02$  by varying  $N_y$  from 500 to 160 000, we found that the results converge only after  $N_y$  is above 50 000. It indicates that indeed large lattice systems are needed in order to explore thermodynamic properties of the Hofstadter model. For higher temperature, the convergence can be reached with smaller  $N_y$ . For the results shown in Figs. 1 and 2, we take  $N_x = 50$  and  $N_y = 80$  000 to ensure convergence. For simplicity, here we only consider the half-filling case, in which the chemical potential is pinned to  $\mu = 0$  because of particle-hole symmetry. In the discussion below, the hopping constant  $t$  is set to 1 and  $\varepsilon = 0.02$ .

Figure 1 shows the quantum oscillation of magnetization at three different temperatures. In the low-field limit, the

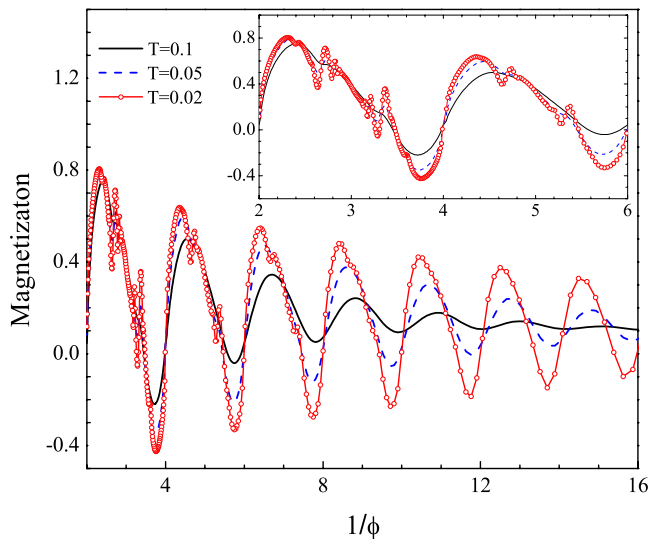


FIG. 1. (Color online) Magnetization of the Hofstadter model at half-filling. The inset shows more clearly the lattice correction to the dHvA oscillation in the high-field regime.

conventional de Haas–van Alphen (dHvA) oscillation is observed. The period of the oscillation  $\Delta(1/\phi)$  is about 2 consistent with the result obtained from the formula<sup>17</sup>  $\Delta(1/\phi) = \frac{4\pi^2}{S_F}$  and  $S_F$  is the Fermi volume. At half filling,  $S_F = 4\pi^2/2 = 2\pi^2$ . However, with increasing  $\phi$ , some subtle structures appear above the conventional dHvA curve expected for two-dimensional electron gas in a magnetic field (see the inset of Fig. 1). These subtle structures become more and more pronounced with decreasing temperature. They result from the lattice correction to the energy spectra.

Thermal fluctuation affects strongly on the line shape of magnetization. At high temperature, say  $T=0.1$ , the fine fractal structure of the Hofstadter butterfly with an energy scale less than  $k_B T$  is smeared out by thermal fluctuation. Only the conventional dHvA oscillation survives, except in the high-field limit. However, at low temperature, say  $T=0.02$ , the fine structures of the Hofstadter butterfly with energy scales

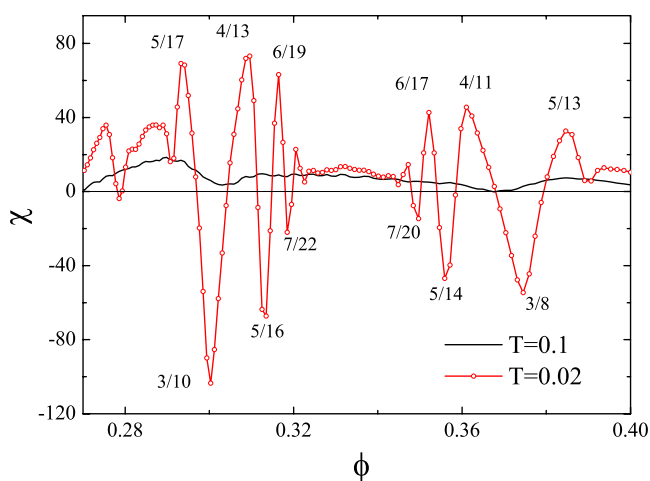


FIG. 2. (Color online) Magnetic susceptibility for the Hofstadter model at half-filling. The values of  $\phi$  corresponding to local maxima and minima in the  $T=0.02$  curve are marked.

comparable to  $k_B T$  will begin to influence the magnetic response of the system. It yields the sharp peaks or dips observed in the magnetization curve in high fields. By further reducing temperature, we found that more and more peaks and dips, even in the low-field range, will emerge from the dHvA background.

Around each sharp peak or dip, there is a change between diamagnetism and paramagnetism with increasing temperature. For example, around  $\phi \sim 0.3$ , the magnetization decreases with increasing  $\phi$  at  $T=0.02$  and the system is diamagnetic; whereas at  $T=0.1$ , the magnetization increases with  $\phi$  and the system is paramagnetic. This change from paramagnetism to diamagnetism is apparently due to the change in energy resolution since the energy spectrum is unchanged. It is a manifestation of the fractal structure of the Hofstadter butterfly.

Figure 2 shows the field dependence of magnetic susceptibility  $\chi$  for  $\phi$  between 0.27 and 0.4 at  $T=0.1$  and 0.02. At high temperature,  $T=0.1$ ,  $\chi$  is paramagnetic. However, at low temperature,  $T=0.02$ ,  $\chi$  oscillates strongly with  $\phi$ . It shows a series of local maxima and minima, at which  $\chi$  is positive (paramagnetic) and negative (diamagnetic), respectively. These extremes appear when the magnetic flux takes some rational values  $\phi=p/q$  (see the rational numbers given in Fig. 2). The maxima and minima correspond to odd and even  $q$ , respectively.

The appearance of these extremes results clearly from the interplay between periodic potential and magnetic field. It is strongly correlated with the density of states of the system at the Fermi level. The density of states was calculated analytically in Ref. 18. At half-filling, the density of states vanishes linearly at the Fermi level (namely, at a Dirac point) when  $q$  is even.<sup>11</sup> However, there is a Van Hove singularity at the Fermi level and the density of states is divergent when  $q$  is odd.<sup>11</sup> Thus the magnetic response is paramagnetic if  $\phi$  is close to a Van Hove singularity and diamagnetic if  $\phi$  is close to a Dirac point.

However, this connection between the extremes and density of states seems fragile if considering that there are infinite rational numbers  $p/q$  with even *and* odd denominators in an arbitrary small but finite interval of  $\phi$ . In other words, near any rational number, say  $\phi=4/13$ , there are infinite other  $\phi$  at which the density of states at the Fermi level can be either zero or divergent. So how can we attribute the orbital paramagnetism at  $4/13$  to the Van Hove singularity in the density of states?

This problem can be resolved by considering the hierarchical structure of the Hofstadter butterfly and the temperature smearing of the band structure. At the first rank of hierarchy, the Hofstadter butterfly is divided into several subcells.<sup>2</sup> These subcells can be further divided recursively into many sub-subcells. This hierarchical recursion defines a parallel iterative transformation. After this transformation, any rational  $\phi$  can be finally reduced to a simple rational number, which is equal to either  $1/q'$  or  $1-1/q'$ , where  $q'$  is an integer.

For example,  $\phi=4/13$  can be reduced to  $4/5$  after only one iteration. This means in the first-order subcell centered at the Fermi level, there are five subbands and the middle one has a divergent density of states crossing the Fermi level. On

the other hand,  $\phi=401/1300$ , which is a value very close to  $4/13$ , can be reduced to  $3/4$  after 19 iterations. This means that in the 19th-order subcell, there are four subbands and the middle two meet at the Fermi level. In this case, the Fermi level is a Dirac point and the corresponding density of states vanishes. However, the characteristic energy scale of the 19th-order subcell is very small compared with the thermal energy  $k_B T$  at  $T=0.02$ . Therefore, the contribution by the singularity at  $\phi=401/1300$  to  $\chi$  is completely smeared out by thermal fluctuation and only the peak at  $\phi=4/13$  can be seen at  $T=0.02$ .

This can be seen more clearly by integrating out the density of states in an interval of  $k_B T$  around the Fermi level. We find that the integral at  $\phi=401/1300$  is hardly different from that at  $\phi=4/13$ . Therefore, around  $\phi\sim 4/13$  the density of states at the Fermi level is determined by the Van Hove singularity in the first subcell at  $4/13$ . A similar argument can be applied to  $\phi$  with even  $q$ . The difference is that in that case, the density of states is dominated by the Dirac points.

The above argument implies that the higher-order subcells of the Hofstadter butterfly can be probed by increasing the energy resolution. Thus more Van Hove singularities and Dirac points can be discerned by lowering the temperature. However, in the limit of zero temperature, the susceptibility

is no longer a well-defined quantity, since it can oscillate between paramagnetism and diamagnetism in an infinitesimally small interval of  $\phi$ . This is consistent with the fact that the ground-state energy is not differentiable with respect to  $\phi$ .

In conclusion, we have introduced a quantum transfer-matrix method to study thermodynamic properties of the Hofstadter model on square lattices. This method allows thermodynamic quantities to be accurately and efficiently evaluated without suffering from the finite-size effect. Our study suggests that the Hofstadter butterfly can be probed by thermodynamic measurements. In particular, the magnetic susceptibility is sensitive to the change in the density of states. It shows a paramagnetic peak if the density of states has a Van Hove singularity at the Fermi level or a diamagnetic dip if the Fermi surface is a Dirac point. Thus the measurement of magnetic susceptibility, which can be materialized on the superlattice<sup>5</sup> or cold atom<sup>19</sup> systems, can reveal not only the fractal structure of spectra but also the density of states of the Hofstadter model.

We thank L. Yu for useful discussions. This work was supported by the NSF-China and the National Program for Basic Research of MOST, China.

\*yanglp@itp.ac.cn

<sup>1</sup>M. Ya. Azbel, Zh. Eksp. Teor. Fiz. **46**, 730 (1964) [Sov. Phys. JETP **19**, 634 (1964)].

<sup>2</sup>D. R. Hofstadter, Phys. Rev. B **14**, 2239 (1976).

<sup>3</sup>D. Langbein, Phys. Rev. **180**, 633 (1969).

<sup>4</sup>D. J. Thouless, M. Kohmoto, M. P. Nightingale, and M. den Nijs, Phys. Rev. Lett. **49**, 405 (1982).

<sup>5</sup>C. Albrecht, J. H. Smet, K. von Klitzing, D. Weiss, V. Umansky, and H. Schweizer, Phys. Rev. Lett. **86**, 147 (2001).

<sup>6</sup>D. Weiss, K. von Klitzing, K. Ploog, and G. Weimann, Europhys. Lett. **8**, 179 (1989); R. R. Gerhardts, D. Weiss, and K. von Klitzing, Phys. Rev. Lett. **62**, 1173 (1989).

<sup>7</sup>U. Kuhl and H. J. Stöckmann, Phys. Rev. Lett. **80**, 3232 (1998).

<sup>8</sup>P. G. Harper, Proc. Phys. Soc., London, Sect. A **68**, 874 (1955).

<sup>9</sup>P. B. Wiegmann and A. V. Zabrodin, Phys. Rev. Lett. **72**, 1890 (1994).

<sup>10</sup>Y. Hatsugai, M. Kohmoto, and Y. S. Wu, Phys. Rev. Lett. **73**,

1134 (1994).

<sup>11</sup>Y. Hasegawa, P. Lederer, T. M. Rice, and P. B. Wiegmann, Phys. Rev. Lett. **63**, 907 (1989).

<sup>12</sup>O. Gat and J. E. Avron, Phys. Rev. Lett. **91**, 186801 (2003).

<sup>13</sup>M. Taut, H. Eschrig, and M. Richter, Phys. Rev. B **72**, 165304 (2005); V. M. Gvozdkov and M. Taut, *ibid.* **75**, 155436 (2007).

<sup>14</sup>H. F. Trotter, Proc. Am. Math. Soc. **10**, 545 (1959).

<sup>15</sup>M. Suzuki, Prog. Theor. Phys. **56**, 1454 (1976).

<sup>16</sup>L. P. Yang, Y. J. Wang, W. H. Xu, M. P. Qin, and T. Xiang, arXiv:0812.0128 (unpublished).

<sup>17</sup>N. W. Ashcroft and N. D. Mermin, *Solid State Physics* (Thomson Learning, Inc., New York, 1976).

<sup>18</sup>G. H. Wannier, G. M. Obermair, and R. Ray, Phys. Status Solidi B **93**, 337 (1979).

<sup>19</sup>R. O. Umucalilar, H. Zhai, and M. Ö. Oktel, Phys. Rev. Lett. **100**, 070402 (2008).